

Precise measurement of the $e^+e^- \rightarrow \pi^+\pi^- J/\psi$ cross section at center-of-mass energies from 3.77 to 4.60 GeV

M. Ablikim¹, M. N. Achasov^{9,e}, S. Ahmed¹⁴, X. C. Ai¹, O. Albayrak⁵, M. Albrecht⁴, D. J. Ambrose⁴⁴, A. Amoroso^{49A,49C}, F. F. An¹, Q. An^{46,a}, J. Z. Bai¹, O. Bakina²³, R. Baldini Ferroli^{20A}, Y. Ban³¹, D. W. Bennett¹⁹, J. V. Bennett⁵, N. Berger²², M. Bertani^{20A}, D. Bettoni^{21A}, J. M. Bian⁴³, F. Bianchi^{49A,49C}, E. Boger^{23,c}, I. Boyko²³, R. A. Briere⁵, H. Cai⁵¹, X. Cai^{1,a}, O. Cakir^{40A}, A. Calcaterra^{20A}, G. F. Cao¹, S. A. Cetin^{40B}, J. Chai^{49C}, J. F. Chang^{1,a}, G. Chelkov^{23,c,d}, G. Chen¹, H. S. Chen¹, J. C. Chen¹, M. L. Chen^{1,a}, S. Chen⁴¹, S. J. Chen²⁹, X. Chen^{1,a}, X. R. Chen²⁶, Y. B. Chen^{1,a}, X. K. Chu³¹, G. Cibinetto^{21A}, H. L. Dai^{1,a}, J. P. Dai³⁴, A. Dbeyssi¹⁴, D. Dedovich²³, Z. Y. Deng¹, A. Denig²², I. Denysenko²³, M. Destefanis^{49A,49C}, F. De Mori^{49A,49C}, Y. Ding²⁷, C. Dong³⁰, J. Dong^{1,a}, L. Y. Dong¹, M. Y. Dong^{1,a}, Z. L. Dou²⁹, S. X. Du⁵³, P. F. Duan¹, J. Z. Fan³⁹, J. Fang^{1,a}, S. S. Fang¹, X. Fang^{46,a}, Y. Fang¹, R. Farinelli^{21A,21B}, L. Fava^{49B,49C}, F. Feldbauer²², G. Felici^{20A}, C. Q. Feng^{46,a}, E. Fioravanti^{21A}, M. Fritsch^{14,22}, C. D. Fu¹, Q. Gao¹, X. L. Gao^{46,a}, Y. Gao³⁹, Z. Gao^{46,a}, I. Garzia^{21A}, K. Goetzen¹⁰, L. Gong³⁰, W. X. Gong^{1,a}, W. Gradl²², M. Greco^{49A,49C}, M. H. Gu^{1,a}, Y. T. Gu¹², Y. H. Guan¹, A. Q. Guo¹, L. B. Guo²⁸, R. P. Guo¹, Y. Guo¹, Y. P. Guo²², Z. Haddadi²⁵, A. Hafner²², S. Han⁵¹, X. Q. Hao¹⁵, F. A. Harris⁴², K. L. He¹, F. H. Heinsius⁴, T. Held⁴, Y. K. Heng^{1,a}, T. Holtmann⁴, Z. L. Hou¹, C. Hu²⁸, H. M. Hu¹, J. F. Hu^{49A,49C}, T. Hu^{1,a}, Y. Hu¹, G. S. Huang^{46,a}, J. S. Huang¹⁵, X. T. Huang³³, X. Z. Huang²⁹, Z. L. Huang²⁷, T. Hussain⁴⁸, W. Ikegami Andersson⁵⁰, Q. Ji¹, Q. P. Ji¹⁵, X. B. Ji¹, X. L. Ji^{1,a}, L. W. Jiang⁵¹, X. S. Jiang^{1,a}, X. Y. Jiang³⁰, J. B. Jiao³³, Z. Jiao¹⁷, D. P. Jin^{1,a}, S. Jin¹, T. Johansson⁵⁰, A. Julin⁴³, N. Kalantar-Nayestanaki²⁵, X. L. Kang¹, X. S. Kang³⁰, M. Kavatsyuk²⁵, B. C. Ke⁵, P. Kiese²², R. Kliemt¹⁰, B. Kloss²², O. B. Kolcu^{40B,h}, B. Kopf⁴, M. Kornicer⁴², A. Kupsc⁵⁰, W. Kühn²⁴, J. S. Lange²⁴, M. Lara¹⁹, P. Larin¹⁴, L. Lavezzi^{49C,1}, H. Leithoff²², C. Leng^{49C}, C. Li⁵⁰, Cheng Li^{46,a}, D. M. Li⁵³, F. Li^{1,a}, F. Y. Li³¹, G. Li¹, H. B. Li¹, H. J. Li¹, J. C. Li¹, Jin Li³², K. Li¹³, K. Li³³, Lei Li³, P. R. Li^{7,41}, Q. Y. Li³³, T. Li³³, W. D. Li¹, W. G. Li¹, X. L. Li³³, X. N. Li^{1,a}, X. Q. Li³⁰, Y. B. Li², Z. B. Li³⁸, H. Liang^{46,a}, Y. F. Liang³⁶, Y. T. Liang²⁴, G. R. Liao¹¹, D. X. Lin¹⁴, B. Liu³⁴, B. J. Liu¹, C. X. Liu¹, D. Liu^{46,a}, F. H. Liu³⁵, Fang Liu¹, Feng Liu⁶, H. B. Liu¹², H. H. Liu¹, H. H. Liu¹⁶, H. M. Liu¹, J. Liu¹, J. B. Liu^{46,a}, J. P. Liu⁵¹, J. Y. Liu¹, K. Liu³⁹, K. Y. Liu²⁷, L. D. Liu³¹, P. L. Liu^{1,a}, Q. Liu⁴¹, S. B. Liu^{46,a}, X. Liu²⁶, Y. B. Liu³⁰, Y. Y. Liu³⁰, Z. A. Liu^{1,a}, Zhiqing Liu²², H. Loehner²⁵, X. C. Lou^{1,a,g}, H. J. Lu¹⁷, J. G. Lu^{1,a}, Y. Lu¹, Y. P. Lu^{1,a}, C. L. Luo²⁸, M. X. Luo⁵², T. Luo⁴², X. L. Luo^{1,a}, X. R. Lyu⁴¹, F. C. Ma²⁷, H. L. Ma¹, L. L. Ma³³, M. M. Ma¹, Q. M. Ma¹, T. Ma¹, X. N. Ma³⁰, X. Y. Ma^{1,a}, Y. M. Ma³³, F. E. Maas¹⁴, M. Maggiora^{49A,49C}, Q. A. Malik⁴⁸, Y. J. Mao³¹, Z. P. Mao¹, S. Marcello^{49A,49C}, J. G. Messchendorp²⁵, G. Mezzadri^{21B}, J. Min^{1,a}, T. J. Min¹, R. E. Mitchell¹⁹, X. H. Mo^{1,a}, Y. J. Mo⁶, C. Morales Morales¹⁴, N. Yu. Muchnoi^{9,e}, H. Muramatsu⁴³, P. Musiol⁴, Y. Nefedov²³, F. Nerling¹⁰, I. B. Nikolaev^{9,e}, Z. Ning^{1,a}, S. Nisar⁸, S. L. Niu^{1,a}, X. Y. Niu¹, S. L. Olsen³², Q. Ouyang^{1,a}, S. Pacetti^{20B}, Y. Pan^{46,a}, P. Patteri^{20A}, M. Pelizaeus⁴, H. P. Peng^{46,a}, K. Peters^{10,i}, J. Pettersson⁵⁰, J. L. Ping²⁸, R. G. Ping¹, R. Poling⁴³, V. Prasad¹, H. R. Qi², M. Qi²⁹, S. Qian^{1,a}, C. F. Qiao⁴¹, L. Q. Qin³³, N. Qin⁵¹, X. S. Qin¹, Z. H. Qin^{1,a}, J. F. Qiu¹, K. H. Rashid⁴⁸, C. F. Redmer²², M. Ripka²², G. Rong¹, Ch. Rosner¹⁴, X. D. Ruan¹², A. Sarantsev^{23,f}, M. Savrie^{21B}, C. Schnier⁴, K. Schoenning⁵⁰, W. Shan³¹, M. Shao^{46,a}, C. P. Shen², P. X. Shen³⁰, X. Y. Shen¹, H. Y. Sheng¹, W. M. Song¹, X. Y. Song¹, S. Sosio^{49A,49C}, S. Spataro^{49A,49C}, G. X. Sun¹, J. F. Sun¹⁵, S. S. Sun¹, X. H. Sun¹, Y. J. Sun^{46,a}, Y. Z. Sun¹, Z. J. Sun^{1,a}, Z. T. Sun¹⁹, C. J. Tang³⁶, X. Tang¹, I. Tapan^{40C}, E. H. Thorndike⁴⁴, M. Tiemens²⁵, I. Uman^{40D}, G. S. Varner⁴², B. Wang³⁰, B. L. Wang⁴¹, D. Wang³¹, D. Y. Wang³¹, K. Wang^{1,a}, L. L. Wang¹, L. S. Wang¹, M. Wang³³, P. Wang¹, P. L. Wang¹, W. Wang^{1,a}, W. P. Wang^{46,a}, X. F. Wang³⁹, Y. Wang³⁷, Y. D. Wang¹⁴, Y. F. Wang^{1,a}, Y. Q. Wang²², Z. Wang^{1,a}, Z. G. Wang^{1,a}, Z. H. Wang^{46,a}, Z. Y. Wang¹, Z. Y. Wang¹, T. Weber²², D. H. Wei¹¹, P. Weidenkaff²², S. P. Wen¹, U. Wiedner⁴, M. Wolke⁵⁰, L. H. Wu¹, L. J. Wu¹, Z. Wu^{1,a}, L. Xia^{46,a}, L. G. Xia³⁹, Y. Xia¹⁸, D. Xiao¹, H. Xiao⁴⁷, Z. J. Xiao²⁸, Y. G. Xie^{1,a}, Yuehong Xie⁶, Q. L. Xiu^{1,a}, G. F. Xu¹, J. J. Xu¹, L. Xu¹, Q. J. Xu¹³, Q. N. Xu⁴¹, X. P. Xu³⁷, L. Yan^{49A,49C}, W. B. Yan^{46,a}, W. C. Yan^{46,a}, Y. H. Yan¹⁸, H. J. Yang^{34,j}, H. X. Yang¹, L. Yang⁵¹, Y. X. Yang¹¹, M. Ye^{1,a}, M. H. Ye⁷, J. H. Yin¹, Z. Y. You³⁸, B. X. Yu^{1,a}, C. X. Yu³⁰, J. S. Yu²⁶, C. Z. Yuan¹, Y. Yuan¹, A. Yuncu^{40B,b}, A. A. Zafar⁴⁸, Y. Zeng¹⁸, Z. Zeng^{46,a}, B. X. Zhang¹, B. Y. Zhang^{1,a}, C. C. Zhang¹, D. H. Zhang¹, H. H. Zhang³⁸, H. Y. Zhang^{1,a}, J. Zhang¹, J. J. Zhang¹, J. L. Zhang¹, J. Q. Zhang¹, J. W. Zhang^{1,a}, J. Y. Zhang¹, J. Z. Zhang¹, K. Zhang¹, L. Zhang¹, S. Q. Zhang³⁰, X. Y. Zhang³³, Y. Zhang¹, Y. Zhang¹, Y. H. Zhang^{1,a}, Y. N. Zhang⁴¹, Y. T. Zhang^{46,a}, Yu Zhang⁴¹, Z. H. Zhang⁶, Z. P. Zhang⁴⁶, Z. Y. Zhang⁵¹, G. Zhao¹, J. W. Zhao^{1,a}, J. Y. Zhao¹, J. Z. Zhao^{1,a}, Lei Zhao^{46,a}, Ling Zhao¹, M. G. Zhao³⁰, Q. Zhao¹, Q. W. Zhao¹, S. J. Zhao⁵³, T. C. Zhao¹, Y. B. Zhao^{1,a}, Z. G. Zhao^{46,a}, A. Zhemchugov^{23,c}, B. Zheng⁴⁷, J. P. Zheng^{1,a}, W. J. Zheng³³, Y. H. Zheng⁴¹, B. Zhong²⁸, L. Zhou^{1,a}, X. Zhou⁵¹, X. K. Zhou^{46,a}, X. R. Zhou^{46,a}, X. Y. Zhou¹, K. Zhu¹, K. J. Zhu^{1,a}, S. Zhu¹, S. H. Zhu⁴⁵, X. L. Zhu³⁹, Y. C. Zhu^{46,a}, Y. S. Zhu¹, Z. A. Zhu¹, J. Zhuang^{1,a}, L. Zotti^{49A,49C}, B. S. Zou¹, J. H. Zou¹

(BESIII Collaboration)

¹ Institute of High Energy Physics, Beijing 100049, People's Republic of China² Beihang University, Beijing 100191, People's Republic of China

- ³ Beijing Institute of Petrochemical Technology, Beijing 102617, People's Republic of China
- ⁴ Bochum Ruhr-University, D-44780 Bochum, Germany
- ⁵ Carnegie Mellon University, Pittsburgh, Pennsylvania 15213, USA
- ⁶ Central China Normal University, Wuhan 430079, People's Republic of China
- ⁷ China Center of Advanced Science and Technology, Beijing 100190, People's Republic of China
- ⁸ COMSATS Institute of Information Technology, Lahore, Defence Road, Off Raiwind Road, 54000 Lahore, Pakistan
- ⁹ G.I. Budker Institute of Nuclear Physics SB RAS (BINP), Novosibirsk 630090, Russia
- ¹⁰ GSI Helmholtzcentre for Heavy Ion Research GmbH, D-64291 Darmstadt, Germany
- ¹¹ Guangxi Normal University, Guilin 541004, People's Republic of China
- ¹² Guangxi University, Nanning 530004, People's Republic of China
- ¹³ Hangzhou Normal University, Hangzhou 310036, People's Republic of China
- ¹⁴ Helmholtz Institute Mainz, Johann-Joachim-Becher-Weg 45, D-55099 Mainz, Germany
- ¹⁵ Henan Normal University, Xinxiang 453007, People's Republic of China
- ¹⁶ Henan University of Science and Technology, Luoyang 471003, People's Republic of China
- ¹⁷ Huangshan College, Huangshan 245000, People's Republic of China
- ¹⁸ Hunan University, Changsha 410082, People's Republic of China
- ¹⁹ Indiana University, Bloomington, Indiana 47405, USA
- ²⁰ (A)INFN Laboratori Nazionali di Frascati, I-00044, Frascati, Italy; (B)INFN and University of Perugia, I-06100, Perugia, Italy
- ²¹ (A)INFN Sezione di Ferrara, I-44122, Ferrara, Italy; (B)University of Ferrara, I-44122, Ferrara, Italy
- ²² Johannes Gutenberg University of Mainz, Johann-Joachim-Becher-Weg 45, D-55099 Mainz, Germany
- ²³ Joint Institute for Nuclear Research, 141980 Dubna, Moscow region, Russia
- ²⁴ Justus-Liebig-Universitaet Giessen, II. Physikalisches Institut, Heinrich-Buff-Ring 16, D-35392 Giessen, Germany
- ²⁵ KVI-CART, University of Groningen, NL-9747 AA Groningen, The Netherlands
- ²⁶ Lanzhou University, Lanzhou 730000, People's Republic of China
- ²⁷ Liaoning University, Shenyang 110036, People's Republic of China
- ²⁸ Nanjing Normal University, Nanjing 210023, People's Republic of China
- ²⁹ Nanjing University, Nanjing 210093, People's Republic of China
- ³⁰ Nankai University, Tianjin 300071, People's Republic of China
- ³¹ Peking University, Beijing 100871, People's Republic of China
- ³² Seoul National University, Seoul, 151-747 Korea
- ³³ Shandong University, Jinan 250100, People's Republic of China
- ³⁴ Shanghai Jiao Tong University, Shanghai 200240, People's Republic of China
- ³⁵ Shanxi University, Taiyuan 030006, People's Republic of China
- ³⁶ Sichuan University, Chengdu 610064, People's Republic of China
- ³⁷ Soochow University, Suzhou 215006, People's Republic of China
- ³⁸ Sun Yat-Sen University, Guangzhou 510275, People's Republic of China
- ³⁹ Tsinghua University, Beijing 100084, People's Republic of China
- ⁴⁰ (A)Ankara University, 06100 Tandogan, Ankara, Turkey; (B)Istanbul Bilgi University, 34060 Eyup, Istanbul, Turkey; (C)Uludag University, 16059 Bursa, Turkey; (D)Near East University, Nicosia, North Cyprus, Mersin 10, Turkey
- ⁴¹ University of Chinese Academy of Sciences, Beijing 100049, People's Republic of China
- ⁴² University of Hawaii, Honolulu, Hawaii 96822, USA
- ⁴³ University of Minnesota, Minneapolis, Minnesota 55455, USA
- ⁴⁴ University of Rochester, Rochester, New York 14627, USA
- ⁴⁵ University of Science and Technology Liaoning, Anshan 114051, People's Republic of China
- ⁴⁶ University of Science and Technology of China, Hefei 230026, People's Republic of China
- ⁴⁷ University of South China, Hengyang 421001, People's Republic of China
- ⁴⁸ University of the Punjab, Lahore-54590, Pakistan
- ⁴⁹ (A)University of Turin, I-10125, Turin, Italy; (B)University of Eastern Piedmont, I-15121, Alessandria, Italy; (C)INFN, I-10125, Turin, Italy
- ⁵⁰ Uppsala University, Box 516, SE-75120 Uppsala, Sweden
- ⁵¹ Wuhan University, Wuhan 430072, People's Republic of China
- ⁵² Zhejiang University, Hangzhou 310027, People's Republic of China

⁵³ Zhengzhou University, Zhengzhou 450001, People's Republic of China

^a Also at State Key Laboratory of Particle Detection and Electronics, Beijing 100049, Hefei 230026, People's Republic of China

^b Also at Bogazici University, 34342 Istanbul, Turkey

^c Also at the Moscow Institute of Physics and Technology, Moscow 141700, Russia

^d Also at the Functional Electronics Laboratory, Tomsk State University, Tomsk, 634050, Russia

^e Also at the Novosibirsk State University, Novosibirsk, 630090, Russia

^f Also at the NRC “Kurchatov Institute”, PNPI, 188300, Gatchina, Russia

^g Also at University of Texas at Dallas, Richardson, Texas 75083, USA

^h Also at Istanbul Arel University, 34295 Istanbul, Turkey

ⁱ Also at Goethe University Frankfurt, 60323 Frankfurt am Main, Germany

^j Also at Institute of Nuclear and Particle Physics, Shanghai Key Laboratory for Particle Physics and Cosmology, Shanghai 200240, People's Republic of China

(Dated: November 7, 2016)

The cross section for the process $e^+e^- \rightarrow \pi^+\pi^- J/\psi$ is measured precisely at center-of-mass energies from 3.77 to 4.60 GeV using 9 fb^{-1} of data collected with the BESIII detector operating at the BEPCII storage ring. Two resonant structures are observed in a fit to the cross section. The first resonance has a mass of $(4222.0 \pm 3.1 \pm 1.4) \text{ MeV}/c^2$ and a width of $(44.1 \pm 4.3 \pm 2.0) \text{ MeV}$, while the second one has a mass of $(4320.0 \pm 10.4 \pm 7.0) \text{ MeV}/c^2$ and a width of $(101.4_{-19.7}^{+25.3} \pm 10.2) \text{ MeV}$, where the first errors are statistical and second ones systematic. The first resonance is near $4.22 \text{ GeV}/c^2$, corresponding to the so-called $Y(4260)$ resonance reported by previous experiments. However, our measured mass is lower and the width is narrower than previous measurements. The second structure is observed in $e^+e^- \rightarrow \pi^+\pi^- J/\psi$ for the first time. The statistical significance is estimated to be larger than 7.6σ .

PACS numbers: 14.40.Rt, 13.25.Gv, 14.40.Pq, 13.66.Bc

The process $e^+e^- \rightarrow \pi^+\pi^- J/\psi$ at center-of-mass (c.m.) energies between 3.8 and 5.0 GeV was first measured by the BABAR experiment using an initial-state-radiation (ISR) technique [1], and a new structure, the $Y(4260)$, was reported with a mass around $4.26 \text{ GeV}/c^2$. This observation was immediately confirmed by the CLEO [2] and Belle experiments [3] in the same process. In addition, the Belle experiment reported an accumulation of events at around 4 GeV, which was called $Y(4008)$ later. Although the $Y(4008)$ state is still controversial — a new measurement by the BABAR experiment does not confirm it [4], while an updated measurement by the Belle experiment still supports its existence [5] — the observation of the Y -states has stimulated substantial theoretical discussions on their nature [6, 7].

Being produced in e^+e^- annihilation, the Y -states have quantum numbers $J^{PC} = 1^{--}$. However, unlike the known 1^{--} charmonium states in the same mass range, such as $\psi(4040)$, $\psi(4160)$ and $\psi(4415)$ [8] which decay predominantly into open charm final states [$D^{(*)}\bar{D}^{(*)}$], the Y states show strong coupling to hidden-charm final states [9]. The observation of the states $Y(4360)$ and $Y(4660)$ in $e^+e^- \rightarrow \pi^+\pi^-\psi(2S)$ [10], together with the $Y(4260)$ in $e^+e^- \rightarrow \pi^+\pi^- J/\psi$ also overpopulate the vector charmonium spectrum predicted by potential models [11]. All of this indicates that the Y states may not be conventional charmonium states, and they are good candidates for new types of exotic particles, such as hybrids, tetraquarks, or meson molecules [6, 7].

The $Y(4260)$ state was once considered a good hybrid candidate [12] since its mass is close to the value predicted by the flux tube model for the lightest hybrid charmonium [13].

Meanwhile, the diquark-antidiquark tetraquark model predicts a wide spectrum of states which can also accommodate the $Y(4260)$ [14]. Moreover, a recent observation of a charged charmoniumlike state $Z_c(3900)$ by BESIII [15], Belle [5] and with CLEO data [16] suggests that the $Y(4260)$ may be a meson molecule candidate [17]. To better identify the nature of the Y states and distinguish various models, more precise experimental measurements, including the production cross section, the mass and width of the Y states, are essential.

In this Letter, we report a precise measurement of the $e^+e^- \rightarrow \pi^+\pi^- J/\psi$ cross section at e^+e^- c.m. energies from 3.77 to 4.60 GeV, using a data sample with an integrated luminosity of 9.05 fb^{-1} [18] collected with the BESIII detector operating at the BEPCII storage ring [19]. The J/ψ candidate is reconstructed with its leptonic decay modes ($\mu^+\mu^-$ and e^+e^-). The data sample used in this measurement includes two independent data sets. A high luminosity data set (dubbed “XYZ data”) contains more than 40 pb^{-1} at each c.m. energy with total integrated luminosity of 8.2 fb^{-1} ; and a low luminosity data set (dubbed “Scan data”) contains about $7\text{--}9 \text{ pb}^{-1}$ at each c.m. energy with a total integrated luminosity of 0.8 fb^{-1} . The integrated luminosities are measured with Bhabha events with an uncertainty of 1% [18]. The c.m. energy of each data sample is measured using dimuon events, with an uncertainty of $\pm 0.8 \text{ MeV}$ [20].

The BESIII detector, described in detail in Ref. [19], has a geometrical acceptance of 93% of the full solid angle. A small-cell helium-based main drift chamber (MDC) provides a charged particle momentum resolution of 0.5% at $1 \text{ GeV}/c$ in a 1 T magnetic field, and supplies energy-loss (dE/dx) mea-

measurements with a resolution better than 6% for electrons from Bhabha scattering. The electromagnetic calorimeter (EMC) measures photon energies with a resolution of 2.5% (5%) at 1 GeV in the barrel (endcaps). Particle identification (PID) is provided by a time-of-flight system (TOF) with a time resolution of 80 ps (110 ps) for the barrel (endcaps). The muon system provides 2 cm position resolution and detects muon tracks with momenta greater than 0.5 GeV/c.

The GEANT4-based [21] Monte Carlo (MC) simulation software package BOOST [22], which includes the geometric description of the BESIII detector and the detector response, is used to optimize event selection criteria, determine the detection efficiency, and estimate the backgrounds. For the signal process, we generate 60,000 $e^+e^- \rightarrow \pi^+\pi^- J/\psi$ events at each c.m. energy of the ‘‘XYZ data’’, and an extrapolation is performed to the ‘‘Scan data’’ with nearby c.m. energies. At e^+e^- c.m. energies between 4.189 and 4.358 GeV, the signal events are generated according to the Dalitz plot distribution obtained from the data sample, since there is significant $Z_c(3900)$ production [5, 15, 16]. At other c.m. energies, signal events are generated using an EVTGEN [23] phase space model. The J/ψ decays into $\mu^+\mu^-$ and e^+e^- with same branching fractions [8]. The ISR is simulated with KKMC [24], and the maximum ISR photon energy is set to correspond to a 3.72 GeV/c² production threshold of the $\pi^+\pi^- J/\psi$ system. Final-state-radiation (FSR) is handled with PHOTOS [25]. Possible background contributions are estimated with KKMC-generated inclusive MC samples with comparable integrated luminosities to the ‘‘XYZ data’’.

Events with four charged tracks with zero net charge are selected. For each charged track, the polar angle in the MDC must satisfy $|\cos\theta| < 0.93$, and the point of closest approach to the e^+e^- interaction point must be within ± 10 cm in the beam direction and within 1 cm in the plane perpendicular to the beam direction. Since pions and leptons are kinematically well separated in the signal decay, charged tracks with momenta larger than 1.06 GeV/c in the laboratory frame are assumed to be leptons, and the others are assumed to be pions. We use the energy deposited in the EMC to separate electrons from muons. For both muon candidates, the deposited energy in the EMC is required to be less than 0.35 GeV, while for both electrons, it is required to be larger than 1.1 GeV. Each event is required to have two pions and two leptons with zero net charge.

To improve the momentum and energy resolution and to reduce the background, a four-constraint (4C) kinematic fit is applied to the event with the hypothesis $e^+e^- \rightarrow \pi^+\pi^-\ell^+\ell^-$ ($\ell = e$ or μ), which constrains the total four-momentum of the final state particles to that of the initial colliding beams. The χ^2 of the kinematic fit is required to be less than 60.

To suppress radiative Bhabha and radiative dimuon ($e^+e^- \rightarrow \gamma e^+e^-/\gamma\mu^+\mu^-$) backgrounds associated with photon conversion to an e^+e^- pair which subsequently is misidentified as a $\pi^+\pi^-$ pair, the cosine of the opening angle of the pion-pair ($\cos\theta_{\pi^+\pi^-}$) candidates is required to be less than 0.98 both for $J/\psi \rightarrow \mu^+\mu^-$ and e^+e^- events. For $J/\psi \rightarrow e^+e^-$ events, since there are more abundant photon

sources from radiative Bhabha events, we further require the cosine of the opening angle of pion-electron pair ($\cos\theta_{\pi^+e^-}$) candidates to be less than 0.98. These requirements remove almost all of the Bhabha and dimuon background events, with an efficiency loss of less than 1% for signal events.

After imposing the above selection criteria, a clear J/ψ signal is observed in the invariant mass distribution of the lepton pairs [$M(\ell^+\ell^-)$]. Using MC simulated events, we estimate a mass resolution of (3.7 ± 0.2) MeV/c² for $J/\psi \rightarrow \mu^+\mu^-$, and (3.9 ± 0.3) MeV/c² for $J/\psi \rightarrow e^+e^-$. The J/ψ mass window is defined as $3.08 < M(\ell^+\ell^-) < 3.12$ GeV/c². In order to estimate the non- J/ψ backgrounds contribution, we also define the J/ψ mass sideband as $3.00 < M(\ell^+\ell^-) < 3.06$ GeV/c² and $3.14 < M(\ell^+\ell^-) < 3.20$ GeV/c², which is three times as wide as the signal region. The dominant background comes from continuum $q\bar{q}$ processes, such as $e^+e^- \rightarrow \pi^+\pi^-\pi^+\pi^-$. Since $q\bar{q}$ events will form a smooth distribution in the J/ψ signal region, their contribution can be either subtracted by a fit to the $M(\ell^+\ell^-)$ distribution, or estimated by the events in the J/ψ sideband region. Contributions from other backgrounds, such as $e^+e^- \rightarrow \eta J/\psi$ [26] are estimated to be negligible according to MC simulations.

In order to determine the signal yields, we make use of both fitting and counting methods on the $M(\ell^+\ell^-)$ distribution. In the ‘‘XYZ data’’, each data set contains many signal events, and an unbinned maximum likelihood fit to the $M(\ell^+\ell^-)$ distribution is performed. We use a MC simulated signal shape convolved with a Gaussian function (to account for the resolution difference between the data and the MC simulation) as the signal probability density function (PDF), and a linear term for the background. For the ‘‘Scan data’’, due to the low statistics, we directly count the number of events in the J/ψ signal region and that of the normalized background events in the J/ψ mass sideband, and take the difference as the signal yields.

The dressed cross section of $e^+e^- \rightarrow \pi^+\pi^- J/\psi$ is calculated using

$$\sigma^{\text{dress}} = \frac{N^{\text{sig}}}{\mathcal{L}_{\text{int}}(1 + \delta)\epsilon\mathcal{B}}, \quad (1)$$

where N^{sig} is the number of signal events, \mathcal{L}_{int} is the integrated luminosity of data, $1 + \delta$ is the ISR correction factor, ϵ is the detection efficiency, and \mathcal{B} is the branching fraction of $J/\psi \rightarrow \ell^+\ell^-$ [8]. The ISR correction factor is obtained using the KKMC [24] program, by incorporating the initial cross section line shape of $e^+e^- \rightarrow \pi^+\pi^- J/\psi$ from published results [4, 5], and then iterating with the measured line shape until it converges. Figure 1 shows the measured dressed cross section from both the ‘‘XYZ data’’ and ‘‘Scan data’’ (Numerical results are listed in the supplemental material [27]).

To study the possible resonant structures in the $e^+e^- \rightarrow \pi^+\pi^- J/\psi$ process, a simultaneous maximum likelihood fit is performed to the measured cross section for both ‘‘XYZ data’’ and ‘‘Scan data’’. For each data set i at c.m. energy \sqrt{s} , the expected number of signal events is $N_i^{\text{exp}} = \sigma_{\text{fit}}(\sqrt{s})\mathcal{L}_{\text{int}}^i(1 + \delta)_i\epsilon_i\mathcal{B}$. For the ‘‘XYZ data’’, the distribution of N_i^{exp} can be

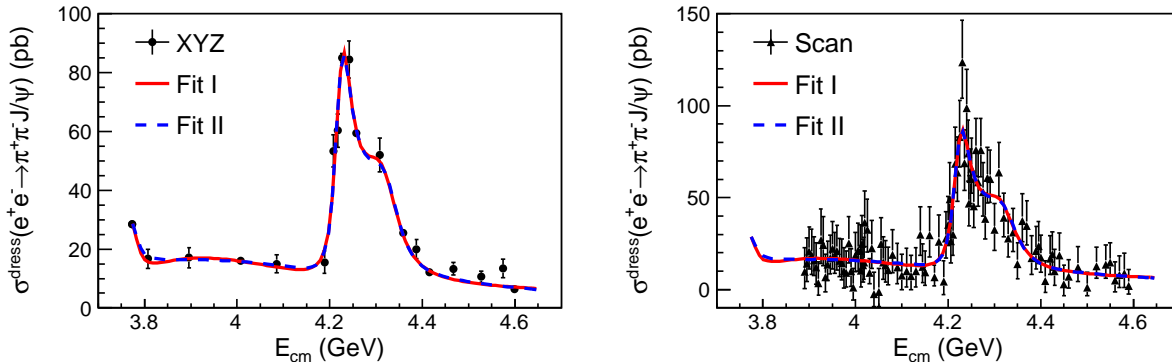


FIG. 1: Measured dressed cross section $\sigma^{\text{dress}}(e^+e^- \rightarrow \pi^+\pi^- J/\psi)$ and simultaneous fit to the “XYZ data” (left) and “Scan data” (right) with the coherent sum of three Breit-Wigner functions (red solid curves) and the coherent sum of an exponential continuum and two Breit-Wigner functions (blue dashed curves). Dots with error bars are data.

well approximated by a Gaussian distribution. The mean and standard deviation of the Gaussian are estimated through a fit to the $M(\ell^+\ell^-)$ distribution of data. For the “Scan data”, the number of events in the J/ψ signal region (including both signal and background) follows a Poisson distribution, with mean value $\mu_i = N_i^{\text{exp}} + N_i^{\text{bkg}}$. Here N_i^{bkg} is the normalized number of background events estimated from the J/ψ mass sideband. The likelihood function is constructed as $\mathcal{L} = \prod_i^{\text{XYZ}} G_i(s|\vec{\theta}) \prod_j^{\text{Scan}} P_j(s|\vec{\theta})$, where $G_i(s|\vec{\theta})$ is a Gaussian distribution which describes the “XYZ data” set i , and $P_j(s|\vec{\theta})$ is a Poisson distribution which describes the “Scan data” set j , and s and $\vec{\theta}$ represent the measured quantities and the fit parameters in the PDF, respectively. The product runs over the full data sets both from the “XYZ data” and the “Scan data”.

We fit to the $e^+e^- \rightarrow \pi^+\pi^- J/\psi$ cross section with the coherent sum of three Breit-Wigner (BW) functions, together with an incoherent $\psi(3770)$ (mass and width are fixed to PDG [8] values) component which accounts for the decay of $\psi(3770) \rightarrow \pi^+\pi^- J/\psi$. Due to the lack of data near the $\psi(3770)$ resonance, it is impossible to determine the relative phase between the $\psi(3770)$ amplitude and the other amplitudes. The BW function to describe a resonance R is written as

$$\text{BW}(\sqrt{s}) = \frac{M \sqrt{12\pi\Gamma_{e^+e^-}\Gamma_{\text{tot}}\mathcal{B}_R}}{\sqrt{s} s - M^2 + iM\Gamma_{\text{tot}}} \sqrt{\frac{\Phi(\sqrt{s})}{\Phi(M)}}, \quad (2)$$

where M , Γ_{tot} and $\Gamma_{e^+e^-}$ are the mass, full width (constant) and electronic width of the resonance R , respectively; \mathcal{B}_R is the branching fraction of the decay $R \rightarrow \pi^+\pi^- J/\psi$; and $\Phi(\sqrt{s})$ is the phase space factor of the three-body decay $R \rightarrow \pi^+\pi^- J/\psi$ [8]. There are four solutions with equally good fit quality and identical masses and widths of the resonances (listed in Table I), while the phase angle and the product of the electronic width with the branching fraction are different (listed in Table II). The resonance R_1 has a mass consistent with that of $Y(4008)$ observed by Belle [3, 5] within errors, but has a larger width. The resonance R_2 corresponds to

the $Y(4260)$ peak reported by *BABAR*, *CLEO* and *Belle* [1–3], but the measured mass $4222.0 \pm 3.1 \text{ MeV}/c^2$ is lower, and its width of $44.1 \pm 4.3 \text{ MeV}$ is much narrower than the $Y(4260)$ parameters reported by previous experiments [1–5]. We also observe a new resonance R_3 with mass $4320.0 \pm 10.4 \text{ MeV}/c^2$ and width $101.4^{+25.3}_{-19.7} \text{ MeV}/c^2$. The statistical significance of R_3 is estimated to be 7.9σ (including systematic uncertainties) by comparing the change of $\Delta(-2 \ln \mathcal{L}) = 74.9$ with and without the R_3 amplitude in the fit, and taking the change of number of degree of freedom $\Delta ndf = 4$ into account. Figure 1 shows the fit results. The fit quality is estimated using a χ^2 -test method, with $\chi^2/ndf = 93.6/110$. Fit methods taken from previous experiments [1–5] are also tried and found to be not able to describe data.

TABLE I: The measured masses and widths of the resonances from the fit to the $e^+e^- \rightarrow \pi^+\pi^- J/\psi$ cross section with three coherent Breit-Wigner functions. The numbers in the brackets correspond to a fit by replacing R_1 with an exponential describing the continuum. The errors are statistical only.

Parameters	Fit result
$M(R_1)$	$3812.6^{+61.9}_{-96.6} (\dots)$
$\Gamma_{\text{tot}}(R_1)$	$476.9^{+78.4}_{-64.8} (\dots)$
$M(R_2)$	$4222.0 \pm 3.1 (4220.9 \pm 2.9)$
$\Gamma_{\text{tot}}(R_2)$	$44.1 \pm 4.3 (44.1 \pm 3.8)$
$M(R_3)$	$4320.0 \pm 10.4 (4326.8 \pm 10.0)$
$\Gamma_{\text{tot}}(R_3)$	$101.4^{+25.3}_{-19.7} (98.2^{+25.4}_{-19.6})$

As an alternative description of the data, we use an exponential $[p_0 e^{-p_1(\sqrt{s}-M_{\text{th}})} \Phi(\sqrt{s})]$, where p_0 and p_1 are free parameters, $M_{\text{th}} = 2m_\pi + m_{J/\psi}$ is the mass threshold of the $\pi^+\pi^- J/\psi$ system, and $\Phi(\sqrt{s})$ the phase space factor] to model the cross section near 4 GeV as in Ref. [4], instead of the resonance R_1 . The fit results are shown as dashed line in Fig. 1. This model also describes data very well. A χ^2 -test to the fit quality gives $\chi^2/ndf = 93.2/111$. Thus, the existence of a resonance near 4 GeV, such as the reso-

TABLE II: The values of $\Gamma_{e^+e^-}\mathcal{B}(R \rightarrow \pi^+\pi^-J/\psi)$ (in eV) from a fit to the $e^+e^- \rightarrow \pi^+\pi^-J/\psi$ cross section. ϕ_1 and ϕ_2 (in degrees) are the phase angles of the resonance R_2 and R_3 . The numbers in the brackets correspond to the fit by replacing resonance R_1 with an exponential to describe the continuum. The errors are statistical only.

Parameters	Solution I	Solution II	Solution III	Solution IV
$\Gamma_{e^+e^-}\mathcal{B}[\psi(3770) \rightarrow \pi^+\pi^-J/\psi]$	0.5 ± 0.1 (0.4 ± 0.1)			
$\Gamma_{e^+e^-}\mathcal{B}(R_1 \rightarrow \pi^+\pi^-J/\psi)$	$8.8_{-2.2}^{+1.5}$ (\dots)	$6.8_{-1.5}^{+1.1}$ (\dots)	$7.2_{-1.5}^{+0.9}$ (\dots)	$5.6_{-1.0}^{+0.6}$ (\dots)
$\Gamma_{e^+e^-}\mathcal{B}(R_2 \rightarrow \pi^+\pi^-J/\psi)$	13.3 ± 1.4 (12.0 ± 1.0)	9.2 ± 0.7 (8.9 ± 0.6)	2.3 ± 0.6 (2.1 ± 0.4)	1.6 ± 0.4 (1.5 ± 0.3)
$\Gamma_{e^+e^-}\mathcal{B}(R_3 \rightarrow \pi^+\pi^-J/\psi)$	21.1 ± 3.9 (17.9 ± 3.3)	$1.7_{-0.6}^{+0.8}$ ($1.1_{-0.4}^{+0.5}$)	$13.3_{-1.8}^{+2.3}$ ($12.4_{-1.7}^{+1.9}$)	$1.1_{-0.3}^{+0.4}$ (0.8 ± 0.3)
ϕ_1	-58 ± 11 (-33 ± 8)	-116_{-10}^{+9} (-81_{-8}^{+7})	65_{-20}^{+24} (81_{-14}^{+16})	8 ± 13 (33 ± 9)
ϕ_2	-156 ± 5 (-132 ± 3)	68 ± 24 (107 ± 20)	-115_{-9}^{+11} (-95_{-5}^{+6})	110 ± 16 (144 ± 14)

nance R_1 or the $Y(4008)$ resonance [3], is not necessary to explain the data. There are four solutions with equally good fit quality and identical masses and widths of the resonances (listed in Table I), while the phase angle and the product of the electronic width with the branching fraction are different (listed in Table II). We observe the resonance R_2 with mass 4220.9 ± 2.9 MeV/ c^2 and width 44.1 ± 3.8 MeV, and the resonance R_3 with mass 4326.8 ± 10.0 MeV/ c^2 and width $98.2_{-19.6}^{+25.4}$ MeV, which agree with the previous fit well within errors. The statistical significance of resonance R_3 in this model is estimated to be 7.6σ (including systematic uncertainties) [$\Delta(-2 \ln \mathcal{L}) = 70.7$, $\Delta ndf = 4$] using the same method as above.

The systematic uncertainty for the cross section measurement mainly comes from uncertainties in the luminosity, efficiencies, radiative correction, background shape and branching fraction. The integrated luminosity of all the data sets are measured using large angle Bhabha scattering events, with an uncertainty of 1% [18]. The uncertainty in the tracking efficiency for high momentum leptons is 1% per track. Pions have momenta that range from 0.1 to 1.06 GeV/ c , and the momentum weighted tracking efficiency uncertainty is also 1% per track. For the kinematic fit, we use a similar method as in Ref. [28] to improve the agreement of the χ^2 distribution between data and MC simulation, and the systematic uncertainty for the kinematic fit is estimated to be 0.6% (1.1%) for $\mu^+\mu^-$ (e^+e^-) events. For the MC simulation of signal events, we use both the $\pi^\pm Z_c(3900)^\mp$ model [5, 15, 16] and the phase space model to describe the $e^+e^- \rightarrow \pi^+\pi^-J/\psi$ process. The efficiency difference between these two models is 3.1%, which is taken as systematic uncertainty due to the decay model.

The efficiency for the other selection criteria, the trigger simulation, the event start time determination and the FSR simulation are quite high ($> 99\%$), and their systematic errors are estimated to be less than 1%. In the ISR correction procedure, we iterate the cross section measurement until $(1 + \delta)\epsilon$ converges. The convergence criterion is taken as the systematic uncertainty due to the ISR correction, which is 1%. We obtain the number of signal events by either fitting or counting events in the $M(\ell^+\ell^-)$ distribution. The background shape is described by a linear distribution. Varying the background shape from a linear shape to a second-order polynomial causes a 1.6% (2.1%) difference for the J/ψ signal yield for the $\mu^+\mu^-$ (e^+e^-) mode, which is taken as the

systematic uncertainty for background shape. The branching fraction of $J/\psi \rightarrow \ell^+\ell^-$ is taken from PDG [8], the errors are 0.6% for both J/ψ decay modes. Assuming all the sources of systematic uncertainty to be independent, the total systematic uncertainties are obtained by adding them in quadrature, resulting in 5.7% for the $\mu^+\mu^-$ mode, and 5.9% for the e^+e^- mode.

In both fit scenarios to the $e^+e^- \rightarrow \pi^+\pi^-J/\psi$ cross section, we observe the resonance R_2 and R_3 with similar masses and widths. Since we can not distinguish the two scenarios from data, we take the difference in mass and width as the systematic uncertainties, i.e. 1.1 (6.8) MeV/ c^2 for the mass and 0.0 (3.2) MeV for the width of R_2 (R_3). The absolute c.m. energy of all the data sets were measured with dimuon events, with an uncertainty of ± 0.8 MeV. Such kind of common uncertainty will propagate only to the masses of the resonances with the same amount, i.e. ± 0.8 MeV/ c^2 . In both fits, the $\psi(3770)$ amplitude was added incoherently. The possible interference effect of $\psi(3770)$ component was investigated by adding it coherently in the fit with various phase angles. The largest deviation of the resonant parameters between the fits with and without interference for the $\psi(3770)$ amplitude are taken as systematic error, which is 0.3 (1.3) MeV/ c^2 for the mass, and 2.0 (9.7) MeV for the width of the R_2 (R_3) resonance. Assuming all the systematic uncertainties are independent, we get the total systematic uncertainties by adding them in quadrature, which is 1.4 (7.0) MeV/ c^2 for the mass, and 2.0 (10.2) MeV for the width of R_2 (R_3), respectively.

In summary, we perform a precise cross section measurement of $e^+e^- \rightarrow \pi^+\pi^-J/\psi$ for c.m. energies from $\sqrt{s} = 3.77$ to 4.60 GeV. Two resonant structures are observed, one with a mass of $(4222.0 \pm 3.1 \pm 1.4)$ MeV/ c^2 and a width of $(44.1 \pm 4.3 \pm 2.0)$ MeV, and the other with a mass of $(4320.0 \pm 10.4 \pm 7.0)$ MeV/ c^2 and a width of $(101.4_{-19.7}^{+25.3} \pm 10.2)$ MeV, where the first errors are statistical and the second ones systematic. The first resonance with a mass near 4.22 GeV corresponds to the $Y(4260)$ resonance reported by BABAR, CLEO and Belle [1–3]. However, we find the mass to be lower and the width to be narrower than the $Y(4260)$ parameters reported by previous experiments [1–5]. The second resonance near 4.32 GeV/ c^2 is observed for the first time in the process $e^+e^- \rightarrow \pi^+\pi^-J/\psi$. Its statistical significance is estimated to be larger than 7.6σ . Finally, we can not confirm the existence of the $Y(4008)$ resonance [3, 5]

from our data, since a continuum term also describes the cross section near 4 GeV equally well.

The fact that the resonant parameters of the $Y(4260)$ from our measurement agree with the structures observed in $e^+e^- \rightarrow \omega\chi_{c0}$ [29] and $e^+e^- \rightarrow \pi^+\pi^-h_c$ [30] by BESIII indicates that the $Y(4260)$ has multiple decay channels and is unlikely to be a hadro-charmonium, which tends to decay only to the core $c\bar{c}$ final state (J/ψ) [31]. The mass of the $Y(4260)$ from our measurement also does not favor a recent lattice calculation (with pion mass ~ 400 MeV/ c^2) for the 1^{--} hybrid state with a mass of 4285 ± 14 MeV/ c^2 [32]. If we interpret this resonance as a tetraquark candidate, the most natural assignment could be the $1^{--} 1P$ state ($[cq]_{S=0}[\bar{c}\bar{q}]_{S=0}$) according to a mass comparison [14]. However, the tetraquark interpretation contradicts its predicted dominant decay to the $D\bar{D}$ final state [9]. The mass of $Y(4260)$ from our measurement is quite close to the $D_s^{*+}D_s^{*-}$ threshold (4224 MeV/ c^2), higher than the $f_0(980)J/\psi$ threshold by about 135 MeV/ c^2 , and lower than the $\bar{D}D_1$ and $D_0\bar{D}^*$ thresholds by about 64 MeV/ c^2 and 100 MeV/ c^2 , respectively. The possibility for a molecule explanation of the above meson pairs [17, 33] needs to be re-examined.

The second resonance near 4.32 GeV/ c^2 has a mass and width comparable to the $Y(4360)$ resonance reported by Belle and BABAR in $e^+e^- \rightarrow \pi^+\pi^-\psi(2S)$ [10]. If we assume it is the same resonance as the $Y(4360)$, we observe a new decay channel of $Y(4360) \rightarrow \pi^+\pi^-J/\psi$ for the first time. The mass of this resonance also agrees well with a tetraquark model interpretation [34], and a hybrid explanation from lattice calculation [35] within errors.

The BESIII collaboration thanks the staff of BEPCII and

the IHEP computing center for their strong support. This work is supported in part by National Key Basic Research Program of China under Contract No. 2015CB856700; National Natural Science Foundation of China (NSFC) under Contracts Nos. 11235011, 11322544, 11335008, 11425524; the Chinese Academy of Sciences (CAS) Large-Scale Scientific Facility Program; the CAS Center for Excellence in Particle Physics (CCEPP); the Collaborative Innovation Center for Particles and Interactions (CICPI); Joint Large-Scale Scientific Facility Funds of the NSFC and CAS under Contracts Nos. U1232201, U1332201; CAS under Contracts Nos. KJCX2-YW-N29, KJCX2-YW-N45; 100 Talents Program of CAS; National 1000 Talents Program of China; INPAC and Shanghai Key Laboratory for Particle Physics and Cosmology; German Research Foundation DFG under Contracts Nos. Collaborative Research Center CRC 1044, FOR 2359; Istituto Nazionale di Fisica Nucleare, Italy; Joint Large-Scale Scientific Facility Funds of the NSFC and CAS under Contract No. U1532257; Joint Large-Scale Scientific Facility Funds of the NSFC and CAS under Contract No. U1532258; Koninklijke Nederlandse Akademie van Wetenschappen (KNAW) under Contract No. 530-4CDP03; Ministry of Development of Turkey under Contract No. DPT2006K-120470; NSFC under Contract No. 11275266; The Swedish Research Council; U. S. Department of Energy under Contracts Nos. DE-FG02-05ER41374, DE-SC-0010504, de-sc0012069, DESC0010118; U.S. National Science Foundation; University of Groningen (RuG) and the Helmholtzzentrum fuer Schwerionenforschung GmbH (GSI), Darmstadt; WCU Program of National Research Foundation of Korea under Contract No. R32-2008-000-10155-0.

-
- [1] B. Aubert *et al.* (BABAR Collaboration), Phys. Rev. Lett. **95**, 142001 (2005).
 [2] Q. He *et al.* (CLEO Collaboration), Phys. Rev. D **74**, 091104(R) (2006).
 [3] C. Z. Yuan *et al.* (Belle Collaboration), Phys. Rev. Lett. **99**, 182004 (2007).
 [4] J. P. Lees *et al.* (BABAR Collaboration), Phys. Rev. D **86**, 051102(R) (2012).
 [5] Z. Q. Liu *et al.* (Belle Collaboration), Phys. Rev. Lett. **110**, 252002 (2013).
 [6] N. Brambilla *et al.*, Eur. Phys. J. C **71**, 1534 (2011).
 [7] H. X. Chen, W. Chen, X. Liu and S. L. Zhu, Phys. Rep. **639**, 1 (2016).
 [8] K. A. Olive *et al.* (Particle Data Group), Chin. Phys. C **38**, 090001 (2014).
 [9] X. H. Mo *et al.*, Phys. Lett. B **640**, 182 (2006).
 [10] B. Aubert *et al.* (BABAR Collaboration), Phys. Rev. Lett. **98**, 212001 (2007); X. L. Wang *et al.* (Belle Collaboration), Phys. Rev. Lett. **99**, 142002 (2007); B. Aubert *et al.* (BABAR Collaboration), Phys. Rev. D **89**, 111103 (2014); X. L. Wang *et al.* (Belle Collaboration), Phys. Rev. D **91**, 112007 (2015).
 [11] E. Eichten *et al.*, Phys. Rev. D **17**, 3090 (1978); **21**, 203 (1980); S. Godfrey and N. Isgur, Phys. Rev. D **32**, 189 (1985).
 [12] F. E. Close, P. R. Page, Phys. Lett. B **628**, 215 (2005); S. L. Zhu, Phys. Lett. B **625**, 212 (2005).
 [13] T. Barnes, F. E. Close, E. S. Swanson, Phys. Rev. D **52**, 9 (1995).
 [14] D. Ebert, R. N. Faustov, V. O. Galkin, Eur. Phys. J. C **58**, 399 (2008).
 [15] M. Ablikim *et al.* (BESIII Collaboration), Phys. Rev. Lett. **110**, 252001 (2013).
 [16] T. Xiao *et al.*, Phys. Lett. B **727**, 366 (2013).
 [17] Q. Wang, C. Hanhart and Q. Zhao, Phys. Rev. Lett. **111**, 132003 (2013).
 [18] M. Ablikim *et al.* (BESIII Collaboration), Chin. Phys. C **39**, 093001 (2015); Chin. Phys. C **37**, 123001 (2013).
 [19] M. Ablikim *et al.* (BESIII Collaboration), Nucl. Instrum. Methods Phys. Res., Sect. A **614**, 345 (2010).
 [20] M. Ablikim *et al.* (BESIII Collaboration), Chin. Phys. C **40**, 063001 (2016).
 [21] S. Agostinelli *et al.* (GEANT4 Collaboration), Nucl. Instrum. Methods A **506**, 250 (2003).
 [22] Z. Y. Deng *et al.*, Chin. Phys. C **30**, 371 (2006).
 [23] D. J. Lange, Nucl. Instrum. Methods Phys. Res., Sect. A **462**, 152 (2001).
 [24] S. Jadach, B. F. L. Ward, and Z. Was, Comput. Phys. Commun. **130**, 260 (2000); Phys. Rev. D **63**, 113009 (2001).
 [25] P. Golonka, and Z. Was, Eur. Phys. J. C **45**, 97 (2006).

- [26] M. Ablikim *et al.* (BESIII Collaboration), Phys. Rev. D **86**, 071101(R) (2012); X. L. Wang *et al.* (Belle Collaboration), Phys. Rev. D **87**, 051101(R) (2013); M. Ablikim *et al.* (BESIII Collaboration), Phys. Rev. D **91**, 112005 (2015).
- [27] See supplemental material at [URL will be inserted by publisher] for a summary of number of signal events, luminosity, and dressed cross section at each energy point.
- [28] M. Ablikim *et al.* (BESIII Collaboration), Phys. Rev. D **87**, 012002 (2013).
- [29] M. Ablikim *et al.* (BESIII Collaboration), Phys. Rev. Lett. **114**, 092003 (2015); Phys. Rev. D **93**, 011102(R) (2016).
- [30] Chang-Zheng Yuan, Chin. Phys. C **38** (2014) 043001; M. Ablikim *et al.* (BESIII Collaboration), arXiv:1610.07044.
- [31] S. Dubynskiy, M. B. Voloshin, Phys Lett. B **666**, 344 (2008).
- [32] L. Liu *et al.* (Hadron Spectrum Collaboration), J. High Energy Phys. **07**, 126 (2012).
- [33] A. M. Torres *et al.*, Phys. Rev. D **80**, 094012 (2009); R. M. Albuquerque, M. Nielsen, Nucl. Phys. A **815**, 53 (2009).
- [34] L. Maiani *et al.*, Phys. Rev. D **72**, 031502 (2005).
- [35] Ying Chen *et al.*, Chin. Phys. C **40**, 081002 (2016).

Appendix

TABLE III: The c.m. energy (\sqrt{s}), integrated luminosity (\mathcal{L}), number of J/ψ signal events (N^{sig}), detection efficiency (ϵ), radiative correction factor ($1 + \delta$) and measured cross section [$\sigma^{\text{dress}}(e^+e^- \rightarrow \pi^+\pi^- J/\psi)$] of “XYZ data”. The first errors are statistical and the second systematic.

\sqrt{s} (GeV)	\mathcal{L} (pb^{-1})	N^{sig}	ϵ	$1 + \delta$	σ^{dress} (pb)
3.7730	2931.8	3093.3 ± 61.5	0.423	0.732	$28.5 \pm 0.6 \pm 1.7$
3.8077	50.5	34.7 ± 6.9	0.396	0.871	$16.7 \pm 3.3 \pm 1.0$
3.8962	52.6	36.1 ± 7.1	0.393	0.856	$17.1 \pm 3.4 \pm 1.0$
4.0076	482.0	325.8 ± 21.7	0.392	0.901	$16.0 \pm 1.1 \pm 1.0$
4.0855	52.6	33.9 ± 6.9	0.374	0.961	$15.0 \pm 3.1 \pm 0.9$
4.1886	43.1	26.9 ± 6.5	0.394	0.858	$15.5 \pm 3.8 \pm 0.9$
4.2077	54.6	114.9 ± 11.6	0.446	0.740	$53.4 \pm 5.4 \pm 3.1$
4.2171	54.1	130.5 ± 12.2	0.458	0.731	$60.3 \pm 5.7 \pm 3.5$
4.2263	1091.7	3853.1 ± 68.1	0.465	0.748	$85.1 \pm 1.5 \pm 4.9$
4.2417	55.6	203.5 ± 15.1	0.453	0.802	$84.4 \pm 6.3 \pm 4.9$
4.2580	825.7	2220.9 ± 53.7	0.444	0.853	$59.5 \pm 1.4 \pm 3.4$
4.3079	44.9	101.7 ± 11.2	0.398	0.917	$52.0 \pm 5.7 \pm 3.0$
4.3583	539.8	621.5 ± 28.8	0.372	1.022	$25.4 \pm 1.2 \pm 1.5$
4.3874	55.2	50.5 ± 8.1	0.331	1.155	$20.0 \pm 3.2 \pm 1.2$
4.4156	1073.6	574.5 ± 28.3	0.302	1.227	$12.1 \pm 0.6 \pm 0.7$
4.4671	109.9	63.4 ± 9.8	0.293	1.240	$13.3 \pm 2.1 \pm 0.8$
4.5271	110.0	50.0 ± 8.8	0.293	1.223	$10.6 \pm 1.9 \pm 0.6$
4.5745	47.7	26.1 ± 6.1	0.281	1.213	$13.4 \pm 3.2 \pm 0.8$
4.5995	566.9	143.4 ± 15.9	0.274	1.205	$6.4 \pm 0.7 \pm 0.4$

TABLE IV: The c.m. energy (\sqrt{s}) and measured cross section [$\sigma^{\text{dress}}(e^+e^- \rightarrow \pi^+\pi^- J/\psi)$] of ‘‘Scan data’’. The first errors are statistical and the second systematic.

\sqrt{s} (GeV)	σ^{dress} (pb)	\sqrt{s} (GeV)	σ^{dress} (pb)	\sqrt{s} (GeV)	σ^{dress} (pb)	\sqrt{s} (GeV)	σ^{dress} (pb)
3.8874	$9.7^{+13.1}_{-9.1} \pm 0.6$	3.8924	$14.3^{+13.8}_{-9.8} \pm 0.8$	3.8974	$20.7^{+13.4}_{-9.3} \pm 1.2$	3.9024	$18.5^{+14.2}_{-10.2} \pm 1.1$
3.9074	$16.0^{+12.8}_{-8.5} \pm 0.9$	3.9124	$12.2^{+13.4}_{-9.2} \pm 0.7$	3.9174	$3.6^{+11.4}_{-6.6} \pm 0.2$	3.9224	$26.9^{+17.1}_{-12.6} \pm 1.6$
3.9274	$24.2^{+15.6}_{-11.1} \pm 1.4$	3.9324	$6.8^{+12.4}_{-8.1} \pm 0.4$	3.9374	$13.5^{+12.7}_{-8.5} \pm 0.8$	3.9424	$17.1^{+12.6}_{-8.6} \pm 1.0$
3.9474	$22.2^{+14.8}_{-11.0} \pm 1.3$	3.9524	$18.0^{+13.0}_{-9.3} \pm 1.0$	3.9574	$21.0^{+13.9}_{-10.4} \pm 1.2$	3.9624	$15.5^{+12.3}_{-8.4} \pm 0.9$
3.9674	$14.4^{+13.2}_{-9.1} \pm 0.8$	3.9724	$9.9^{+12.7}_{-9.0} \pm 0.6$	3.9774	$9.2^{+11.7}_{-7.9} \pm 0.5$	3.9824	$25.2^{+14.5}_{-10.8} \pm 1.5$
3.9874	$10.0^{+12.1}_{-8.4} \pm 0.6$	3.9924	$1.0^{+10.5}_{-6.6} \pm 0.1$	3.9974	$18.5^{+12.7}_{-8.9} \pm 1.1$	4.0024	$21.2^{+14.9}_{-11.0} \pm 1.2$
4.0074	$21.0^{+14.3}_{-10.2} \pm 1.2$	4.0094	$10.4^{+13.3}_{-8.9} \pm 0.6$	4.0114	$25.0^{+15.3}_{-10.9} \pm 1.4$	4.0134	$13.3^{+13.8}_{-9.2} \pm 0.8$
4.0154	$14.8^{+13.6}_{-9.3} \pm 0.9$	4.0174	$36.5^{+17.2}_{-13.0} \pm 2.1$	4.0224	$32.7^{+16.6}_{-12.2} \pm 1.9$	4.0274	$9.1^{+7.7}_{-6.0} \pm 0.5$
4.0324	$22.3^{+15.2}_{-10.9} \pm 1.3$	4.0374	$-2.4^{+11.7}_{-7.0} \pm 0.1$	4.0474	$-1.2^{+12.6}_{-8.0} \pm 0.1$	4.0524	$24.8^{+14.4}_{-10.2} \pm 1.4$
4.0574	$14.7^{+13.9}_{-9.2} \pm 0.9$	4.0624	$13.3^{+13.4}_{-9.2} \pm 0.8$	4.0674	$10.7^{+12.3}_{-8.2} \pm 0.6$	4.0774	$19.1^{+13.6}_{-9.9} \pm 1.1$
4.0874	$12.2^{+12.9}_{-9.1} \pm 0.7$	4.0974	$7.5^{+11.7}_{-7.6} \pm 0.4$	4.1074	$9.9^{+12.6}_{-8.5} \pm 0.6$	4.1174	$7.2^{+11.2}_{-7.3} \pm 0.4$
4.1274	$10.0^{+12.7}_{-8.5} \pm 0.6$	4.1374	$29.8^{+15.1}_{-11.1} \pm 1.7$	4.1424	$12.4^{+12.5}_{-8.6} \pm 0.7$	4.1474	$9.5^{+11.4}_{-7.3} \pm 0.6$
4.1574	$29.4^{+15.5}_{-11.8} \pm 1.7$	4.1674	$6.8^{+6.5}_{-4.8} \pm 0.4$	4.1774	$26.0^{+14.4}_{-10.2} \pm 1.5$	4.1874	$4.4^{+11.2}_{-7.0} \pm 0.3$
4.1924	$27.7^{+14.6}_{-10.6} \pm 1.6$	4.1974	$35.3^{+15.5}_{-11.5} \pm 2.0$	4.2004	$49.1^{+19.9}_{-15.6} \pm 2.8$	4.2034	$26.4^{+15.9}_{-11.9} \pm 1.5$
4.2074	$29.7^{+15.1}_{-11.1} \pm 1.7$	4.2124	$69.2^{+19.8}_{-16.1} \pm 4.0$	4.2174	$64.3^{+19.5}_{-15.9} \pm 3.7$	4.2224	$83.7^{+20.0}_{-16.6} \pm 4.9$
4.2274	$124.5^{+22.9}_{-19.7} \pm 7.2$	4.2324	$69.4^{+18.2}_{-15.0} \pm 4.0$	4.2374	$99.4^{+21.4}_{-18.0} \pm 5.8$	4.2404	$74.7^{+18.3}_{-15.2} \pm 4.3$
4.2424	$47.0^{+15.5}_{-12.3} \pm 2.7$	4.2454	$60.5^{+16.5}_{-13.5} \pm 3.5$	4.2474	$66.3^{+16.6}_{-13.5} \pm 3.8$	4.2524	$45.7^{+14.7}_{-11.7} \pm 2.7$
4.2574	$75.9^{+17.1}_{-14.3} \pm 4.4$	4.2624	$58.2^{+15.9}_{-12.9} \pm 3.4$	4.2674	$75.6^{+17.2}_{-14.3} \pm 4.4$	4.2724	$53.0^{+16.0}_{-13.0} \pm 3.1$
4.2774	$38.4^{+14.1}_{-11.0} \pm 2.2$	4.2824	$60.5^{+16.6}_{-13.6} \pm 3.5$	4.2874	$60.1^{+15.7}_{-12.8} \pm 3.5$	4.2974	$32.4^{+14.3}_{-11.1} \pm 1.9$
4.3074	$64.0^{+16.4}_{-13.3} \pm 3.7$	4.3174	$39.1^{+13.3}_{-10.4} \pm 2.3$	4.3274	$27.9^{+13.2}_{-10.0} \pm 1.6$	4.3374	$31.0^{+13.3}_{-10.2} \pm 1.8$
4.3474	$14.0^{+11.4}_{-8.2} \pm 0.8$	4.3574	$37.5^{+14.8}_{-11.6} \pm 2.2$	4.3674	$34.8^{+13.7}_{-10.6} \pm 2.0$	4.3774	$17.1^{+12.2}_{-8.9} \pm 1.0$
4.3874	$20.5^{+13.2}_{-9.6} \pm 1.2$	4.3924	$23.8^{+13.2}_{-9.5} \pm 1.4$	4.3974	$17.5^{+12.1}_{-8.2} \pm 1.0$	4.4074	$4.7^{+11.0}_{-6.2} \pm 0.3$
4.4174	$16.9^{+12.3}_{-8.6} \pm 1.0$	4.4224	$19.1^{+12.4}_{-8.6} \pm 1.1$	4.4274	$9.9^{+11.9}_{-7.6} \pm 0.6$	4.4374	$18.7^{+12.1}_{-8.4} \pm 1.1$
4.4474	$3.0^{+10.2}_{-6.4} \pm 0.2$	4.4574	$6.9^{+9.4}_{-6.1} \pm 0.4$	4.4774	$12.2^{+11.2}_{-7.7} \pm 0.7$	4.4974	$1.0^{+8.3}_{-4.3} \pm 0.1$
4.5174	$12.7^{+10.2}_{-6.7} \pm 0.7$	4.5374	$13.6^{+10.6}_{-7.5} \pm 0.8$	4.5474	$14.7^{+10.8}_{-7.4} \pm 0.9$	4.5574	$4.9^{+10.0}_{-6.2} \pm 0.3$
4.5674	$7.8^{+10.6}_{-6.8} \pm 0.5$	4.5774	$8.7^{+11.1}_{-7.5} \pm 0.5$	4.5874	$2.0^{+8.7}_{-4.4} \pm 0.1$		